

# Comparison of digital signal-signal beat interference compensation techniques in direct-detection subcarrier modulation systems

ZHE LI,\* M. SEZER ERKILINÇ, LIDIA GALDINO, KAI SHI, BENN C. THOMSEN, POLINA BAYVEL, AND ROBERT I. KILLEY

*Optical Networks Group, Department of Electronic and Electrical Engineering, University College London (UCL), London, WC1E 7JE, UK*

\*zhe.li@ee.ucl.ac.uk

**Abstract:** Single-polarization direct-detection transceivers may offer advantages compared to digital coherent technology for some metro, back-haul, access and inter-data center applications since they offer low-cost and complexity solutions. However, a direct-detection receiver introduces nonlinearity upon photo detection, since it is a square-law device, which results in signal distortion due to signal-signal beat interference (SSBI). Consequently, it is desirable to develop effective and low-cost SSBI compensation techniques to improve the performance of such transceivers. In this paper, we compare the performance of a number of recently proposed digital signal processing-based SSBI compensation schemes, including the use of single- and two-stage linearization filters, an iterative linearization filter and a SSBI estimation and cancellation technique. Their performance is assessed experimentally using a  $7 \times 25$  Gb/s wavelength division multiplexed (WDM) single-sideband 16-QAM Nyquist-subcarrier modulation system operating at a net information spectral density of 2.3 (b/s)/Hz.

© 2016 Optical Society of America

**OCIS codes:** (060.0060) Fiber optics and optical communications; (060.2360) Fiber optics links and subsystems.

## References and links

1. Alcatel-Lucent, "Bell Labs metro network traffic growth: architecture impact study," Strategic White Paper (2013).
2. Cisco, "Cisco visual networking index: forecast and methodology, 2014-2019," White Paper (2015).
3. D. Che, Q. Hu, and W. Shieh, "Linearization of direct detection optical channels using self-coherent subsystems," *J. Lightwave Technol.* **34**(2), 516–524 (2016).
4. R. I. Killey, M. S. Erkilinç, Z. Li, S. Pachnicke, H. Griesser, R. Bouziane, B. C. Thomsen, and P. Bayvel, "Spectrally-efficient direct-detection WDM transmission system," in *International Conference on Transparent Optical Networks (ICTON 2015)*, paper We.B3.2.
5. B. J. C. Schmidt, A. J. Lowery, and L. B. Du, "Low sample rate transmitter for direct-detection optical OFDM," in *Optical Fiber Communication Conference, OSA Technical Digest Series (CD)* (Optical Society of America, 2009), paper OWM4.
6. A. O. Wiberg, B.-E. Olsson, and P. A. Andrekson, "Single cycle subcarrier modulation," in *Optical Fiber Communication Conference, OSA Technical Digest Series (CD)* (Optical Society of America, 2009), paper OTuE.1.
7. J. C. Cartledge and A. S. Karar, "100 Gb/s intensity modulation and direct detection," *J. Lightwave Technol.* **32**(16), 2809–2814 (2014).
8. M. S. Erkilinç, Z. Li, S. Pachnicke, H. Griesser, B. C. Thomsen, P. Bayvel, and R. I. Killey, "Spectrally-efficient WDM Nyquist-pulse-shaped 16-QAM subcarrier modulation transmission with direct detection," *J. Lightwave Technol.* **33**(15), 3147–3155 (2015).
9. W. R. Peng, I. Morita, and H. Tanaka, "Enabling high capacity direct-detection optical OFDM transmissions using beat interference cancellation receiver," in *European Conference and Exhibition on Optical Communication (ECOC 2010)*, paper Tu.4.A.2.
10. S. A. Nezamalhossseini, L. R. Chen, Q. Zhuge, M. Malekiha, F. Marvasti, and D. V. Plant, "Theoretical and experimental investigation of direct detection optical OFDM transmission using beat interference cancellation receiver," *Opt. Express* **21**(13), 15237–15246 (2013).
11. J. Ma, "Simple signal-to-signal beat interference cancellation receiver based on balanced detection for a single-sideband optical OFDM signal with a reduced guard band," *Opt. Lett.* **38**(21), 4335–4338 (2013).

12. S. Randel, D. Pileri, S. Chandrasekhar, G. Raybon, and P. Winzer, "100-Gb/s discrete-multitone transmission over 80-km SSMF using single-sideband modulation with novel interference-cancellation scheme," in *European Conference and Exhibition on Optical Communication (ECOC 2015)*, paper Mo.4.5.2.
13. K. Zou, Y. Zhu, F. Zhang, and Z. Chen, "Spectrally efficient terabit optical transmission with Nyquist 64-QAM half-cycle subcarrier modulation and direct detection," *Opt. Lett.* **41**(12), 2767–2770 (2016).
14. Z. Li, M. S. Erkilinc, R. Maher, L. Galdino, K. Shi, B. C. Thomsen, P. Bayvel, and R. I. Killey, "Two-stage linearization filter for direct-detection subcarrier modulation," *IEEE Photonics Technol. Lett.* **28**(24), 2838–2841 (2016).
15. Z. Li, M. S. Erkilinc, R. Maher, L. Galdino, K. Shi, B. C. Thomsen, P. Bayvel, and R. I. Killey, "Reach enhancement for WDM direct-detection subcarrier modulation using low-complexity two-stage signal-signal beat interference cancellation," in *European Conference and Exhibition on Optical Communication (ECOC 2016)*, paper M 2.B.1.
16. W. R. Peng, X. Wu, K. M. Feng, V. R. Arbab, B. Shamee, J. Y. Yang, L. C. Christen, A. E. Willner, and S. Chi, "Spectrally efficient direct-detected OFDM transmission employing an iterative estimation and cancellation technique," *Opt. Express* **17**(11), 9099–9111 (2009).
17. J.-H. Yan, Y.-W. Chen, B.-C. Tsai, and K.-M. Feng, "A multiband DDO-OFDM System with spectral efficient iterative SSBI reduction DSP," *IEEE Photonics Technol. Lett.* **28**(2), 119–122 (2016).
18. Z. Li, M. S. Erkilinc, S. Pachnicke, H. Griesser, R. Bouziane, B. C. Thomsen, P. Bayvel, and R. I. Killey, "Signal-signal beat interference cancellation in spectrally-efficient WDM direct-detection Nyquist-pulse-shaped 16-QAM subcarrier modulation," *Opt. Express* **23**(18), 23694–23709 (2015).
19. C. Sánchez, B. Ortega, and J. Capmany, "System performance enhancement with pre-distorted OOFDM signal waveforms in DM/DD systems," *Opt. Express* **22**(6), 7269–7283 (2014).
20. C. Ju, X. Chen, N. Liu, and L. Wang, "SSII cancellation in 40 Gbps VSB-IMDD OFDM system based on symbol pre-distortion," in *European Conference and Exhibition on Optical Communication (ECOC 2014)*, paper P.7.9.
21. Z. Li, M. S. Erkilinc, R. Bouziane, B. C. Thomsen, P. Bayvel, and R. I. Killey, "Simplified DSP-based signal-signal beat interference mitigation technique for direct detection OFDM," *J. Lightwave Technol.* **34**(3), 866–872 (2016).
22. H.-Y. Chen, C.-C. Wei, H.-H. Chu, Y.-C. Chen, I.-C. Lu, and J. Chen, "An EAM-based 50 Gbps 60-km OFDM system with 29-dB loss budget enabled by SSII cancellation or volterra filter," in *European Conference and Exhibition on Optical Communication (ECOC 2014)*, paper P.3.21.
23. L. Zhang, T. Zuo, Y. Mao, Q. Zhang, E. Zhou, G. N. Liu, and X. Xu, "Beyond 100-Gb/s transmission over 80-km SMF using direct-detection SSB-DMT at C-band," *J. Lightwave Technol.* **34**(2), 723–729 (2016).
24. C. Y. Wong, S. Zhang, L. Liu, T. Wang, Q. Zhang, Y. Fang, S. Deng, G. N. Liu, and X. Xu, "56 Gb/s direct detected single-sideband DMT transmission over 320-km SMF using silicon IQ modulator," in *Optical Fiber Communication Conference, OSA Technical Digest Series (CD)* (Optical Society of America, 2015), paper Th4A.3.
25. R. I. Killey, P. M. Watts, V. Mikhailov, M. Glick, and P. Bayvel, "Electronic dispersion compensation by signal predistortion using digital processing and a dual-drive Mach-Zehnder modulator," *IEEE Photonics Technol. Lett.* **17**(3), 714–716 (2005).
26. R. A. Shafik, M. S. Rahman, and A. R. Islam, "On the extended relationships among EVM, BER and SNR as performance metrics," in *International Conference on Electrical and Computer Engineering (ICECE 2006)*, paper 408–411.
27. S. L. Jansen, I. Morita, and H. Ranaka, "Carrier-to-signal power ratio in fiber-optics SSB-OFDM transmission systems," in *Institute of Electronics, Information and Communication Engineers Conference (IEICE 2007)*, paper B-10–24.

## 1. Introduction

The total data traffic in short- and medium-haul optical links/networks, spanning distances of up to several hundred kilometers, is rapidly increasing, with the largest drivers for the continuous growth being video-on-demand and data centers/cloud applications. Recent studies [1,2] have reported that the metro traffic is growing almost twice as rapidly as the traffic traversing the core/backbone networks, with the majority of the bandwidth being terminated within the metro networks. To cope with this growth, cost-effective optical transceivers offering low power consumption, resilience to noise and fiber impairments, and high information spectral density (ISD) play a key role. In contrast to polarization-multiplexed digital coherent systems, the simple and potentially lower cost of the optical hardware structure of single-polarization direct-detection (DD) wavelength division multiplexing (WDM) systems may make them a favorable solution for inter-data center, access, and metropolitan links/networks, provided they can meet the above-mentioned requirements [3,4].

Subcarrier modulation (SCM) signal formats, in particular orthogonal frequency division multiplexing (OFDM) [5] and Nyquist-pulse shaped subcarrier modulation (Nyquist-SCM) [6–8], can be utilized to achieve high ISDs for DD systems. However, their performance is severely degraded because of a nonlinear effect introduced by the square-law detection, referred to as signal-signal beat interference (SSBI). Since the SSBI products appear over a bandwidth equal to that of the original subcarrier modulated signal ( $B_{sc}$ ), leaving a sufficient spectral guard-band ( $B_{gap} \geq B_{sc}$ ) between the optical carrier and the subcarrier modulated signal can be a solution to avoid the SSBI penalty [5]. However, the achievable ISD is halved and approximately 50% of the electrical and optical components' bandwidths are wasted. Therefore, it is essential to develop effective and low-cost SSBI compensation techniques for future high capacity and spectrally-efficient DD-based wavelength-division-multiplexing (WDM) short- and medium-haul transmission systems.

Recently, a number of SSBI compensation techniques have been investigated for single-polarization DD SCM systems, operating either optically [9–11] or digitally [12–24]. The optical schemes offer superior compensation gain, but have the drawback of increasing the optical transceiver complexity. On the other hand, a number of promising digital compensation schemes have been proposed: the single-stage linearization filter first proposed in [12] enables the mitigation of SSBI using a very simple digital signal processing (DSP) architecture. Its compensation performance can be further improved by iteratively repeating the linearization process or adding an extra linearization stage, techniques termed iterative linearization filter [13] and two-stage linearization filter [14], respectively. Alternatively, in order to maximize the potential compensation gain, especially at high values of optical signal-to-noise power ratio (OSNR), combined linearization and SSBI estimation and cancellation was proposed and investigated in [15] in which the SSBI is estimated from the symbol decisions and subtracted from the received signal waveform. The use of linearization in the latter scheme avoids the complexity of iterative signal demodulation and modulation stages, as proposed in [16–18].

A key question concerns how the performance of these different compensation schemes compare. Published studies of the different techniques have been carried out using a variety of link parameters and signal formats, making such comparisons difficult. To address this, in this paper we present a theoretical and experimental assessment of the SSBI compensation schemes using a single system configuration, allowing direct comparisons of their performance. The paper is organized as follows: In Section 2, we analyze the working principles of these four SSBI compensation techniques. Section 3 describes our experimental setup to assess the performance of such techniques in a spectrally-efficient (net information spectral density (ISD) = 2.34 (b/s/Hz)  $7 \times 25$  Gb/s WDM DD single-sideband (SSB) 16-QAM Nyquist-SCM system. In section 4, we report both the experimental back-to-back and transmission results for these four techniques. The obtained experimental results show a good match with the theoretical analysis.

## 2. Working principles of signal-signal beat interference mitigation schemes

This section describes the working principles and mathematical models of the four SSBI compensation schemes being assessed: the single-stage linearization filter, the iterative linearization filter, the two-stage linearization filter and the SSBI estimation and cancellation technique, and discusses their potential advantages and disadvantages.

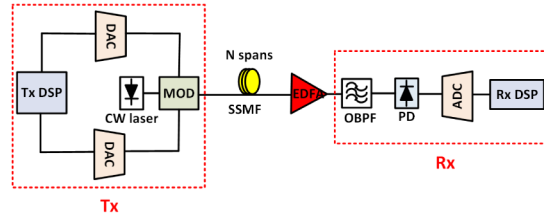


Fig. 1. Schematic diagram of the direct-detection system architecture. Tx & Rx DSP: Transmitter and receiver DSP, DAC: Digital-to-analog converter, MOD: Modulator, SSMF: Standard single-mode fiber, EDFA: Erbium-doped fiber amplifier, OBPF: Optical band-pass filter, PD: Photodiode, ADC: Analog-to-digital converter.

The schematic diagram of the direct-detection system architecture we consider is shown in Fig. 1. In the transmitter DSP, the SSB subcarrier modulated signal,  $E_s(n)$ , is generated by modulation DSP (MOD DSP), where  $n$  is the discrete time index. Afterwards, digital transmitter-based electronic dispersion compensation (EDC) [25] and pre-emphasis are implemented to mitigate the accumulated dispersion of the fiber and the low-pass filtering effects of the transceiver electronics. Following D/A conversion, E/O conversion is carried out, during which the real-valued optical carrier,  $E_{carrier}$ , is added to the SSB SCM signal by optimally biasing the IQ modulator. Following the fiber transmission, direct detection and A/D conversion, the detected double-sideband (DSB) signal after direct current (DC) offset removal,  $V_{DD}(n)$ , can be written as:

$$\begin{aligned} V_{DD}(n) &= K \left[ |E_{carrier} + E_s(n)|^2 \right] \\ &= 2 \operatorname{Re} \left[ E_{carrier} \cdot E_s(n) \right] + |E_s(n)|^2 \end{aligned} \quad (1)$$

where  $K[\cdot]$  signifies the DC offset removal operator, and  $\operatorname{Re}[x]$  represents the real part of  $x$ . In the RHS of this equation, the first term is the desired carrier-signal beating products (CSBP), and the second term is the unwanted SSBI penalty. Following this, the SSBI compensation scheme is applied to  $V_{DD}(n)$ , using one of the approaches described in the following four sections.

### 2.1 Single-stage linearization filter

A single-stage linearization filter has been demonstrated for DD OFDM systems [12], with the receiver DSP design shown in Fig. 2.

#### Rx DSP:

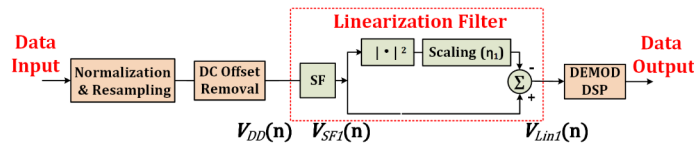


Fig. 2. Receiver DSP design with single-stage linearization filter. SF: sideband filter. DEMOD DSP: SSB SCM signal demodulation.

The detected DSB signal,  $V_{DD}(n)$ , is passed through the linearization filtering stage: a SSB signal is first generated using a sideband filter (SF), and an approximation of the signal-signal beating products is calculated based on the filtered SSB signal, which is then subtracted from the original SSB signal to partially compensate the SSBI. Note that, this technique aims to replicate the process of generating signal-signal beating products from the transmitted SSB signal. The use of the SF avoids unwanted beating products which would otherwise be generated by the negative frequency part of the detected DSB signal spectrum. The signal

after the SF,  $V_{SF1}(n)$ , and the output of the single-stage linearization filter,  $V_{Lin1}(n)$ , are written as follows [14]:

$$V_{SF1}(n) = \alpha \cdot E_s(n) + \Lambda \left[ |E_s(n)|^2 \right] \quad (2)$$

$$\begin{aligned} V_{Lin1}(n) &= V_{SF1}(n) - \eta_l \cdot |V_{SF1}(n)|^2 \\ &= \alpha \cdot E_s(n) + \Lambda \left[ |E_s(n)|^2 \right] - \alpha^2 \eta_l \cdot |E_s(n)|^2 \\ &\quad - 2\alpha \eta_l \cdot \text{Re} \left[ E_s(n)^* \cdot \Lambda \left[ |E_s(n)|^2 \right] \right] - \eta_l \cdot \left[ \Lambda \left[ |E_s(n)|^2 \right] \right]^2 \end{aligned} \quad (3)$$

where  $\alpha$  is an amplitude scaling factor proportional to the optical carrier value,  $\Lambda[\cdot]$  is the SF operator, and  $\eta_l$  is a second amplitude scaling factor which controls the effectiveness of the linearization filter. In the RHS of Eq. (3), the first term is the desired SSB CSBP; since we only demodulate the signal spectrum in the positive frequency domain, the second term (SSBI) can be partially eliminated by the third term with the optimum adjustment of  $\eta_l$ . On the other hand, since the fourth (signal-SSBI beating) and fifth (SSBI-SSBI beating) terms are relatively low, the nonlinear penalty is reduced with respect to the case without implementing this single-stage linearization filter [14].

The advantage of this filter design is its use of a very simple DSP structure. However, as shown in Eq. (2), as the calculation of the signal-signal beating products is based on the received distorted signal, this technique itself introduces extra unwanted beating interference, thus limiting the compensation gain.

## 2.2 Iterative linearization filter

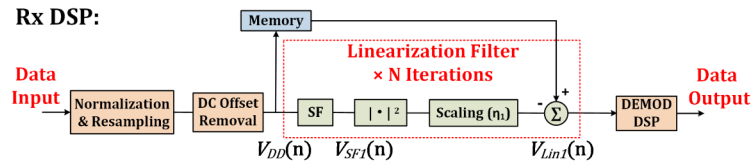


Fig. 3. Receiver DSP design with iterative linearization filter.

To further improve the performance of the single-stage linearization filter, an iterative linearization filter was proposed for DD Nyquist-SCM system in [13]. Figure 3 shows the receiver DSP design with this technique, and its working principle is described as follows: the waveform of  $V_{DD}(n)$  is stored in memory, and the signal-signal beating products are calculated based on the filtered SSB signal, which are then subtracting from the stored signal waveform,  $V_{DD}(n)$ , in the memory, to mitigate the SSBI. It can be seen that if no iterative update is carried out, this technique is the same as the process in the single-stage linearization filter, as described in section 2.1. Since the signal-signal beating products are approximated by  $|V_{SF1}(n)|^2$ , though, as shown in Eq. (2), inaccuracies occur due to the inclusion of the SSBI term in  $V_{SF1}(n)$ . However, this process can be repeated multiple times in order to reduce the inaccuracies and achieve the maximum compensation gain.

This iterative linearization filtering technique improves the performance of the single-stage linearization filter by using the stored received signal waveform and iteratively repeating the SSBI estimation. Due to the multiple (four times or more) iterations performed, the DSP complexity is significantly increased, however.

### 2.3 Two-stage linearization filter

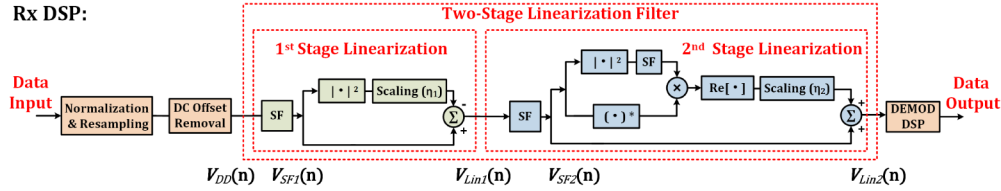


Fig. 4. Receiver DSP design with two-stage linearization filter.

An alternative method to enhance the performance of the single-stage linearization filter is to use a two-stage linearization filter, which was first proposed for DD Nyquist-SCM systems in [14]. The receiver DSP design is shown in Fig. 4. A second linearization stage is applied to remove the majority of the unwanted beating interference introduced by the first stage. Its operating principle can be described as follows: In the first stage, which is the same as the single-stage linearization filter described in section 2.1, with optimum adjustment of  $\eta_1$ , the SSBI penalty is removed and the remaining terms are the signal-SSBI (fourth term) and SSBI-SSBI (fifth) beating terms, as described in Eq. (3). Following this, the signal passes through the second linearization stage to compensate the signal-SSBI beating interference introduced by the first stage, as follows:

$$V_{SF2}(n) = \alpha \cdot E_s(n) - 2\alpha\eta_1 \cdot \Lambda \left[ \text{Re} \left[ E_s(n)^* \cdot \Lambda \left[ |E_s(n)|^2 \right] \right] \right] \quad (4)$$

$$-\eta_1 \cdot \Lambda \left[ \Lambda \left[ |E_s(n)|^2 \right]^2 \right] \quad (5)$$

$$V_{Lin2}(n) = V_{SF2}(n) + \eta_2 \cdot \text{Re} \left[ V_{SF2}(n)^* \cdot \Lambda \left[ |V_{SF2}(n)|^2 \right] \right]$$

where  $V_{SF2}(n)$  is the filtered SSB signal, and  $V_{Lin2}(n)$  is the output of the second linearization stage. The scaling factor  $\eta_2$  can be optimized to achieve the maximum compensation gain. Since the input of the second linearization stage  $V_{Lin2}(n)$  is mainly the desired CSBP, the estimation of the signal-SSBI beating is significantly improved and the majority of the signal-SSBI beating interference can be compensated in this stage, thus further enhancing the compensation performance. It is worth noting that, since the SSBI-SSBI beating term results in a very small penalty in contrast to the signal-SSBI beating term, it is left uncompensated in order to keep the DSP simple.

In contrast to the single-stage linearization filter, the two-stage linearization filter offers the advantage of enhanced compensation performance. Compared with the other digital SSBI compensation schemes such as the above-mentioned iterative linearization filter (section 2.2) or the SSBI estimation and cancellation that will be described in the following section, this technique avoids the requirement for multiple iterations or multiple modulation and demodulation DSP operations. Hence, although the DSP complexity is more than twice that of the single-stage filter, it is still relatively low compared to the other approaches.

### 2.4 Signal-signal beat interference estimation and cancellation

A digital iterative SSBI compensation scheme was proposed for both OFDM [16,17] and Nyquist-SCM [18]. Since multiple iterations and symbol decision making can improve the accuracy of the SSBI approximation, it offers the highest compensation gain at high OSNR values. However, its digital hardware complexity is greatly increased due to the need to perform multiple (typically three or four) signal demodulation and modulation operations in the receiver DSP. Recently, we proposed and demonstrated an SSBI compensation scheme

which is an updated version of the iterative scheme, combining single-stage linearization filter with non-iterative SSBI estimation and cancellation [15]. Results of simulation and experimental studies indicated that it offers compensation performance matching the iterative scheme.

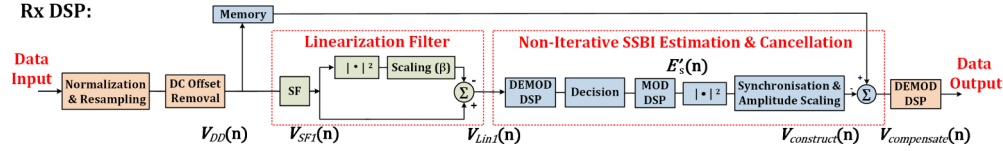


Fig. 5. Receiver DSP design with SSBI estimation and cancellation technique. MOD & DEMOD DSP: SSB SCM signal generation and demodulation.

Figure 5 shows the receiver DSP design with the SSBI estimation and cancellation technique. A detailed description of the technique is given in [15]. Two copies of the detected DSB signal waveform  $V_{DD}(n)$  are made with one being stored in memory and the other being passed through the single-stage linearization filter to partially eliminate the SSBI terms. Following this, non-iterative SSBI estimation and cancellation is performed as follows: A digital representation of the SSB SCM signal, denoted as  $E'_s(n)$ , is generated by modulation DSP (MOD DSP) and an approximation of the signal-signal beating products  $V_{construct}(n)$  is re-constructed, and then subtracted from the stored signal waveform  $V_{DD}(n)$  which can be written as follows:

$$V_{construct}(n) = |E'_s(n)|^2 \quad (6)$$

Since the symbol decisions are significantly more accurate due to the preceding single-stage linearization filtering stage, multiple iterations of the signal demodulation and modulation are not required. Assuming  $E'_s(n) \approx E_s(n)$ , the compensated signal  $V_{compensate}(n)$  can be written as follows:

$$\begin{aligned} V_{compensate}(n) &= V_{DD}(n) - V_{construct}(n) \\ &\approx 2 \operatorname{Re}[E_{carrier} \cdot E_s(n)] \end{aligned} \quad (7)$$

As a result, the effect of SSBI is almost fully eliminated and the compensated signal only contains the desired CSBP. Compared with the linearization filtering schemes, no additional unwanted beating products are introduced. At the same time, since the technique is based on symbol decisions, it also avoids the noise enhancement (signal-ASE and ASE-ASE beating products) which occurs in the linearization filtering schemes. Therefore, it offers potentially better compensation performance. However, the limitation of this technique is its dependency on the accuracy of the symbol decision making, thus noticeably degrading its performance at lower OSNR values.

### 3. Experimental setup

To test and compare the four SSBI compensation schemes described above, transmission experiments were carried out using the optical transmission test-bed shown in Fig. 6. It consists of a  $7 \times 25$  Gb/s SSB 16-QAM Nyquist-SCM transmitter, an optical fiber recirculating loop and a direct-detection receiver to demultiplex and detect the channel of interest.

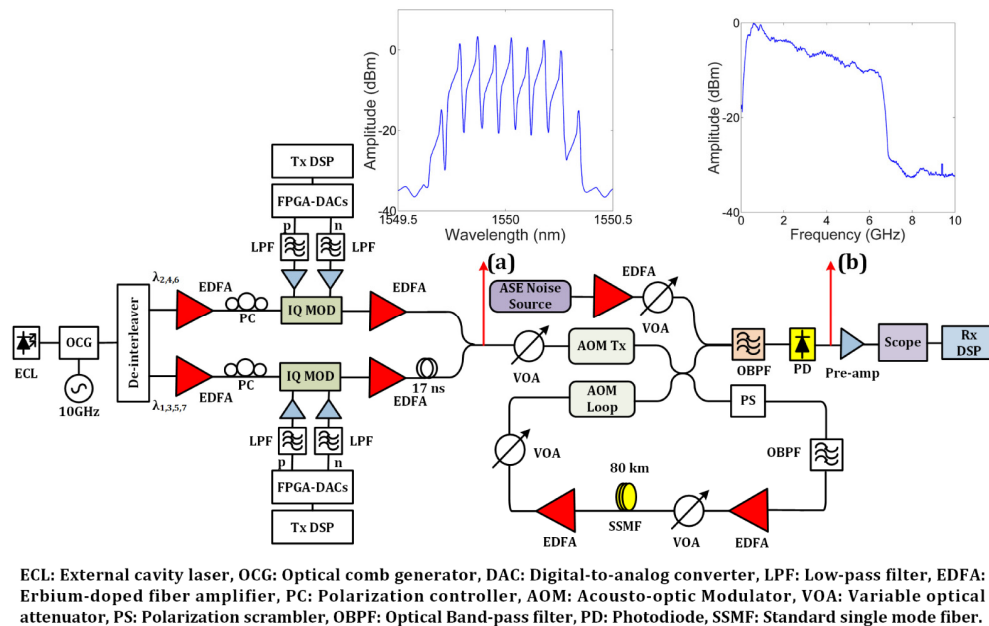


Fig. 6. Experimental test-bed for WDM DD SSB 16-QAM Nyquist-SCM transmission. Insets: (a) Experimental WDM spectrum, (b) Detected digital spectrum.

The principles of the modulation and demodulation of the SCM signals, and the experimental set-up are described in detail in [18], the only differences in this study being that a lower subcarrier frequency of 3.43 GHz (0.55 times the symbol rate) and a roll-off factor of 0.1 for the root-raised cosine pulse shaping and matched filters and a lower WDM channel spacing of 10 GHz were used. The parameters of the optical recirculating fiber loop are listed in Table 1.

Table 1. Parameters of loop components and fiber span

Parameter	Value
fiber length per span ( $L_{span}$ )	80 km
fiber attenuation ( $\alpha$ )	0.2 dB/km
dispersion parameter at reference wavelength ( $D$ )	17 ps/(nm·km)
nonlinear parameter ( $\gamma$ )	1.2 /(W·km)
total loss within the loop	31 dB
EDFA output power	18 dBm
EDFA noise figure	4.5 dB

The system performance was quantified by bit-error-ratio (BER), obtained by error counting, and measurement of the error-vector-magnitude (EVM) [26] over  $2^{18}$  bits. It is worth noting that, the optimization of the optical carrier-to-signal power ratio (CSPR) is crucial to achieve the optimum performance in DD systems. In the experiment, the optical carrier was generated by biasing the IQ-modulators above the null point and the biases were adjusted to achieve the desired CSPR values at a given optical signal-to-noise ratio (OSNR), while the radio frequency (RF) voltage swing was kept constant (3.4V).

#### 4. Results and discussions

The performance of both optical back-to-back and WDM transmission implementing the four SSBI cancellation techniques was assessed using the experimental test-bed described above.

#### 4.1 Optical back-to-back performance

The optical back-to-back performance was evaluated by amplified spontaneous emission (ASE) noise loading at the receiver. The BER curves versus OSNR at 0.1 nm resolution bandwidth for cases of without and with the SSBI cancellation schemes are plotted in Fig. 7.

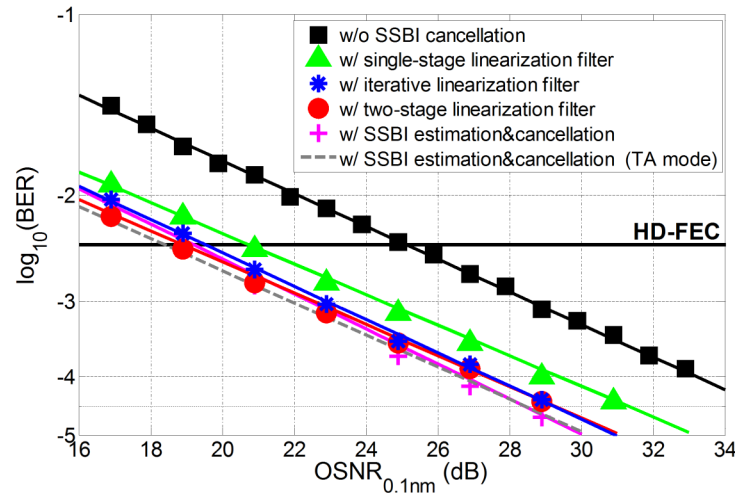


Fig. 7. Experimental BER versus OSNR without and with different digital SSBI post-compensation schemes in back-to-back operation.

The optimum system performance was achieved by sweeping the CSPR value from 6 to 14 dB and adjusting it at each OSNR level. It can be observed that the system performance was significantly improved when the SSBI cancellation methods were performed. The required OSNR value at the hard-decision forward error correction (HD-FEC) threshold ( $\text{BER} = 3.8 \times 10^{-3}$ ) was found to be 25.3 dB without SSBI cancellation, reducing to 21.0 dB using the single-stage linearization filter (4.3 dB gain), 19.6 dB using the iterative linearization filter (5.7 dB gain), 19.2 dB using the SSBI estimation and cancellation (6.1 dB gain) and finally, 18.9 dB (6.4 dB gain) using the two-stage linearization filter schemes. Among these four schemes, the two-stage linearization filter offered the maximum compensation gain at the HD-FEC threshold. Due to accurate approximation of the signal-signal beating terms, the SSBI estimation and cancellation scheme provides the best compensation performance at high OSNRs, although its performance is noticeably degraded at lower OSNR levels due to increased number of inaccurate symbol decisions. In addition, to test the impact of symbol decision making accuracy on the compensation performance, the SSBI estimation and cancellation scheme was also evaluated in a training-assisted (TA) mode, in which a known training sequence is transmitted. In this case, decision errors are avoided when reconstructing the signal-signal beating products. Further compensation gain can be observed especially at lower OSNR levels compared to the case of the practical system in which symbol decision errors cause inaccuracies in the reconstructed signal-signal beating products. This curve, while not achievable in a practical system, represents a lower bound on the BER achievable with DSP-based SSBI compensation. The additional penalties observed with the linearization filters can be explained by their introduction of unwanted beating interference and their noise enhancement.

In order to observe the trade-off between the SSBI and carrier-ASE beating noise before and after applying the SSBI cancellation, the experimental BER curves with respect to the CSPR at six different OSNR values (without and with the two-stage linearization filter scheme) are plotted in Figs. 8(a) and 8(b). They clearly show that the SSBI cancellation leads to improvements in the BERs, and, at the same time, to a reduction in the optimum CSPR

value by approximately 3 dB. Moreover, the dependence of the system performance on OSNR value is reduced when it is SSBI-limited, which matches with the theoretical analysis in [27].

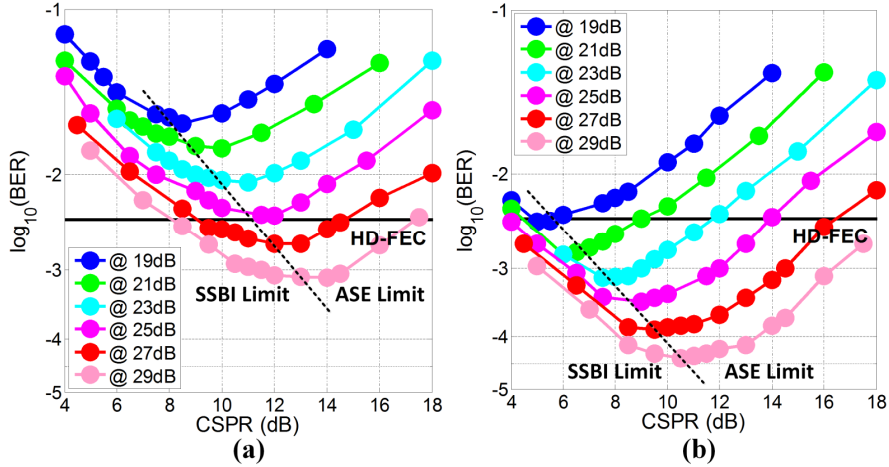


Fig. 8. Experimental BER versus CSPR at different OSNRs (a) without and (b) with two-stage linearization filter in back-to-back operation. The dashed black line indicates the shift of the optimum CSPR value.

Furthermore, an assessment of the dependence of the optimum CSPR value on the OSNR level using each SSBI compensation technique was carried out by plotting the optimum CSPR as a function of OSNR, as shown in Fig. 9. The optimum CSPR value increases with the OSNR, as expected. In comparison to the uncompensated case, the optimum CSPR values need to be reduced by 2 dB for single-stage linearization filter and approximately 3 dB for iterative linearization filters. For SSBI estimation and cancellation scheme, since the compensation effectiveness relies on the accuracy of symbol decision making, the reduction is 3 dB for high OSNRs ( $\geq 23$  dB), gradually reducing to 2 dB for low OSNRs ( $< 21$  dB). For the SSBI estimation and cancellation scheme in training-assisted mode, the reduction of the optimum CSPR was found to be 3.5 dB for all values of OSNR. The BER versus OSNR results in Fig. 7 were obtained at the optimum CSPR values obtained from these results.

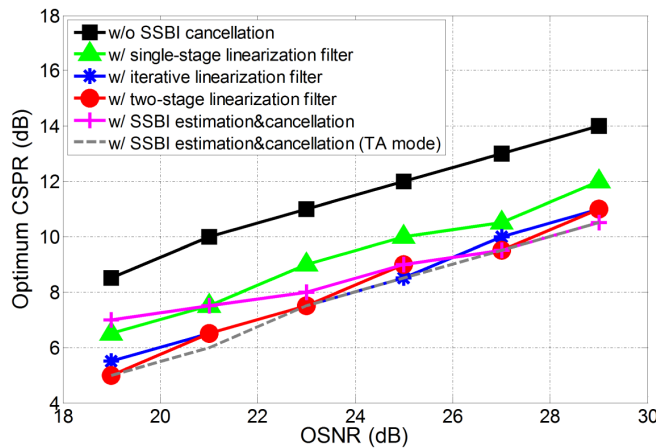


Fig. 9. Experimental optimum CSPR versus OSNR without and with different digital SSBI post-compensation schemes in back-to-back operation.

## 4.2 WDM transmission

Following the assessment of back-to-back performance, WDM transmission experiments over distances of 240 km and 480 km of uncompensated standard single-mode fiber (SSMF) were carried out using the optical test-bed shown in Fig. 6. The optimum CSPR values were found to be 15 dB without and 12-13 dB with SSBI compensation for 240 km transmission, while for 480 km transmission, the corresponding values were 13 dB without and 10-11 dB with SSBI compensation. The BER versus optical launch power per WDM channel without and with the four SSBI mitigation schemes at 240 km and 480 km are shown in Figs. 10 and 11, respectively. It can be observed that the achieved BERs were significantly decreased by implementing the SSBI cancellation schemes.

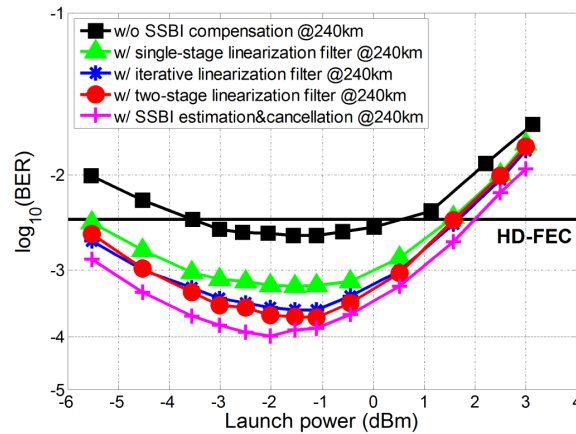


Fig. 10. Experimental BER versus optical launch power per channel at 240 km WDM transmission without and with different digital SSBI post-compensation schemes.

For WDM transmission over 240 km, as shown in Fig. 10, the optimum launch power per channel was reduced by 0.5 dB for the single-stage, iterative, and two-stage linearization filtering approaches, and reduced by 1 dB for SSBI estimation and cancellation. The minimum BER at the optimum launch power reduced from  $2.7 \times 10^{-3}$  without SSBI cancellation to  $7.0 \times 10^{-4}$  with the linearization filter, further decreasing to  $2.5 \times 10^{-4}$  and  $2.0 \times 10^{-4}$  with iterative and two-stage linearization filtering techniques, respectively. The lowest BER was found to be  $1.0 \times 10^{-4}$  when the SSBI estimation and cancellation scheme was used.

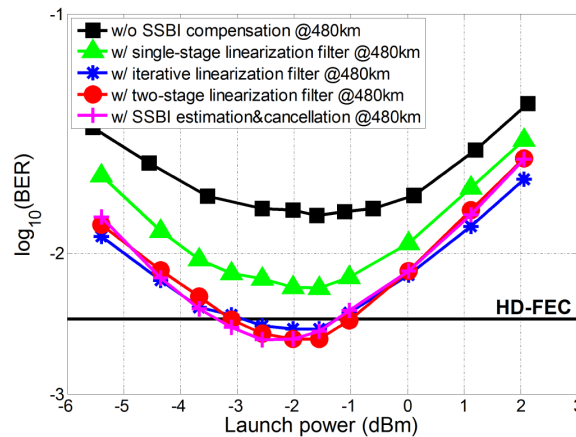


Fig. 11. Experimental BER versus optical launch power per channel at 480 km WDM transmission without and with different digital SSBI post-compensation schemes.

Figure 11 shows the WDM transmission performance over 480 km of SSMF. A 0.5 dB reduction in the optimum launch power per channel was observed when using the single-stage, iterative, and two-stage linearization filtering schemes, compared with a 1 dB reduction whilst using the SSBI estimation and cancellation approach. The minimum BER at the optimum launch power reduced from  $1.6 \times 10^{-2}$  without SSBI compensation to  $6.2 \times 10^{-3}$  with single-stage linearization filter and further decreased to  $3.2 \times 10^{-3}$ ,  $3.0 \times 10^{-3}$  and  $2.6 \times 10^{-3}$  with iterative linearization filter, SSBI estimation and cancellation and two-stage linearization filter, respectively. In contrast to 240 km transmission, it can be observed that the performance of the two-stage linearization filter surpasses the SSBI estimation and cancellation scheme, becoming the best performing of the four compensation schemes. This is mainly because the performance of the SSBI estimation and cancellation scheme was affected by inaccurate symbol decision making at 480 km transmission, due to the lower OSNR. Note that the reduction in gain of all SSBI compensation methods at the longer distances is due to fiber nonlinearity dominating the transmission performance.

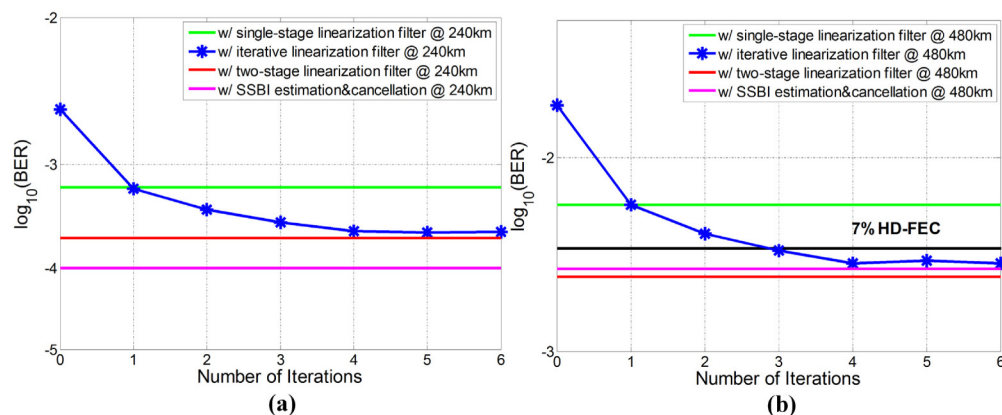


Fig. 12. Experimental BER versus the receiver iteration numbers for the WDM transmission over transmission distances of (a) 240 km and (b) 480 km.

The WDM transmission performance of these SSBI compensation approaches can be further compared from the plots of BER versus applied number of iterations in the iterative linearization filtering approach, shown in Fig. 12, which, it can be seen, requires multiple (approximately four) iterations to achieve the maximum compensation gain, hence causing a significant increase in DSP complexity.

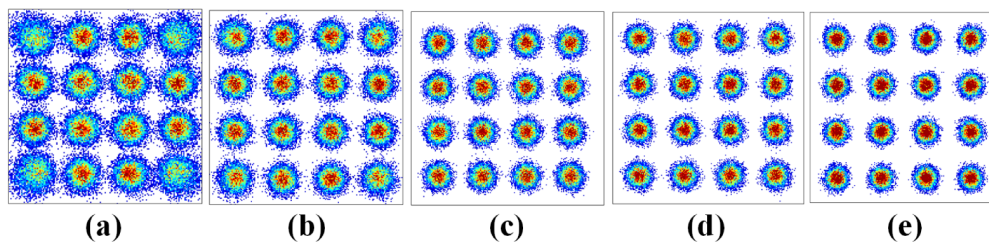


Fig. 13. Received constellation diagrams (a) without (EVM = 17.9%) and with (b) single-stage linearization filter (EVM = 15.7%), (c) iterative linearization filter (EVM = 13.2%), (d) two-stage linearization filter (EVM = 13.0%) and (e) SSBI estimation and cancellation (EVM = 12.4%) after WDM transmission over 240 km.

To clearly observe the compensation performance using these four SSBI compensation techniques, the received constellation diagrams for the transmission over 240 km and 480 km

are presented in Figs. 13 and 14 with the corresponding error vector magnitudes (EVMs) listed in the captions.

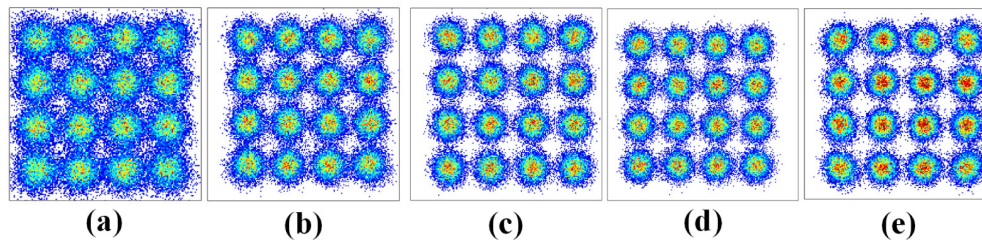


Fig. 14. Received constellation diagrams (a) without (EVM = 22.1%) and with (b) single-stage linearization filter (EVM = 19.2%), (c) iterative linearization filter (EVM = 17.9%), (d) two-stage linearization filter (EVM = 17.4%) and (e) SSBI estimation and cancellation (EVM = 17.6%) after WDM transmission over 480 km.

Finally, for both 240 km and 480 km transmissions, the performance of all seven WDM channels was measured at the optimum launch power per channel, without and with these four cancellation schemes, as shown in Figs. 15(a) and 15(b). Assuming 7% HD-FEC overhead, the net bit-rate per channel was 23.4 Gb/s (a gross bit rate of 25 Gb/s) and the achieved optical net ISD was 2.34 (b/s)/Hz (a gross optical ISD of 2.5 (b/s)/Hz).

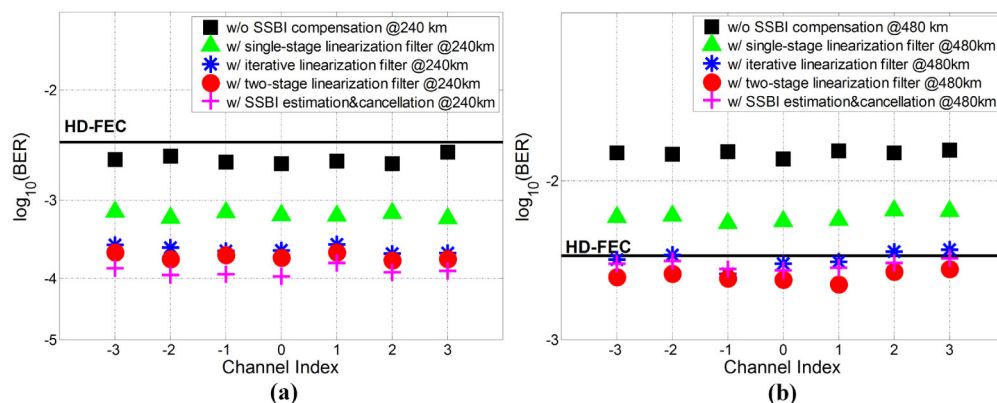


Fig. 15. BER for each received WDM channel without and with different digital SSBI post-compensation schemes over (a) 240 km and (b) 480 km WDM transmissions.

While this paper has presented a comprehensive comparison of the performance of the four compensation schemes, further work will be required to compare, in detail, the computational complexity of the different techniques.

## 5. Conclusion

A joint theoretical and experimental assessment of four promising digital receiver-based signal-signal beat interference (SSBI) compensation techniques (single-stage, iterative, two-stage linearization filters and SSBI estimation and cancellation) was reported, for the first time. The use of a single experimental link design to assess all these schemes allowed a detailed side-by-side comparison of their performance. According to the theoretical analysis and experimental evaluations, we found that the single-stage linearization filter has the simplest DSP complexity but suffers from the problem of the introduction of unwanted beating interference products by the filter itself. This problem can be solved by either repeating this linearization filtering process iteratively to improve the SSBI approximation or adding an extra linearization stage to compensate the majority of the beating interference introduced by the first linearization stage. Experimental results show noticeable improvement

after applying either of these two techniques. Alternatively, the single-stage linearization filter can be combined with a non-iterative SSBI estimation and cancellation stage, which, as its SSBI estimation is based on symbol decisions, potentially offers the best performance at high OSNR values. It was found that the latter scheme does indeed offer the best performance at higher OSNR values, but that the simpler two stage linearization filtering scheme works best at low OSNRs.

**Funding**

European Union ERA-NET+ project, UK EPSRC UNLOC EP/J017582/1 project, EU FP7 ASTRON project, and Semtech Corporation.